







Performance of Cryogenic Adsorbents for Use in Methane Bulk and Clumped Isotope Analysis

¹Department of Earth and Planetary Sciences, ETH Zurich, Zürich, Switzerland | ²Laboratory for Air Pollution/Environmental Technology, Empa, Dübendorf, Switzerland | ³Geological Institute, RWTH Aachen, Aachen, Germany

Correspondence: Nico Kueter (nico.kueter@eaps.ethz.ch; kueter@geol.rwth-aachen.de)

Received: 24 January 2025 | Revised: 17 March 2025 | Accepted: 28 March 2025

Funding: This work was supported by Schweizerischer Nationalfonds zur Förderung der Wissenschaftlichen Forschung, 200021-200977, 206021_183294 and European Metrology Programme for Innovation and Research, 21GRD04.

Keywords: adsorbent | clumped isotopes | laser spectroscopy | methane | sample purification | vapor pressure isotope effect

ABSTRACT

Rationale: Cryogenic trapping of methane is essential for bulk and clumped isotope analyses, requiring adsorbent materials that enable efficient recovery and preserve isotopic signatures. This study evaluates the performance – capacity, isotopic fractionation, and ease of use – of silica gels, zeolite molecular sieves, and activated carbon under various trapping and desorption conditions. A focus is set on the preservation of methane clumped isotope signatures.

Methods: A well-characterized methane reference gas (40 mL) was cryofocused at 77 K in containers filled with silica gels, zeolite molecular sieves (5A and 13X), or activated carbon alongside non-loaded containers. After loading, the containers were warmed in a water bath (21°C–95°C) for various dwell times. The bulk (δ D-CH₄ and δ ¹³C-CH₄) and clumped (Δ ¹³CH₃D and Δ ¹²CH₂D₂) isotopic composition of the desorbed methane were measured against the untreated reference gas using novel quantum cascade laser absorption spectroscopy (QCLAS).

Results: The best results were achieved with coarse-grained (1–3 mm) silica gels heated to 50°C for at least 5 min or at 21°C–22°C for a minimum of 120 min. Elevated desorption temperatures (80°C–95°C) compromised clumped isotope signatures. Although effective for gas trapping, zeolite molecular sieves, and activated carbon introduced significant bulk and clumped isotopic shifts due to catalytic effects and chromatographic isotopologue separation. Methane cryofocused without adsorbents retained its bulk and clumped isotopic composition without significant fractionation.

Conclusions: Among the tested adsorbents, silica gels demonstrated superior performance, preserving $\delta^{13}\text{C-CH}_4$, $\delta\text{D-CH}_4$, $\Delta^{13}\text{CH}_3\text{D}$, and $\Delta^{12}\text{CH}_2\text{D}_2$ values close to or within performance targets while offering high adsorption capacity, reproducibility, and ease of regeneration. Adsorbent-free cryotrapping is a viable alternative for sufficiently large methane volumes, where vapor pressure isotope effects (VPIEs) become negligible. However, cryogenic adsorbents remain indispensable for ensuring isotopic accuracy for small sample volumes and high-precision applications.

1 | Introduction

Analyses of methane bulk (δ^{13} C-CH₄ and δ D-CH₄) and doubly substituted ("clumped": Δ^{12} CH₂D₂ and Δ^{13} CH₃D) isotopes are

relevant in a broad range of prospective applications because they provide a wealth of information, e.g., about formation and equilibrium temperatures, or source and sink processes (e.g., [1–3]). Prior to sample analysis by either high-resolution isotope

[Correction added on 29 September, after first online publication: The copyright line was changed.]

This is an open access article under the terms of the Creative Commons Attribution License, which permits use, distribution and reproduction in any medium, provided the original work is properly cited.

© 2025 The Author(s). Rapid Communications in Mass Spectrometry published by John Wiley & Sons Ltd.

ratio mass spectrometry (HR-IRMS) or quantum cascade laser absorption spectroscopy (QCLAS) [4–8], matrix effects and the low abundance of rare isotopologues necessitate $\mathrm{CH_4}$ preconcentration and cryofocusing. Numerous manual and automated purification methods have been developed, all incorporating cryogenic separation steps [4, 9–11].

Typically, methane is cryofocused using activated carbon (AC), zeolite molecular sieves (MS), or silica gel (SG) at temperatures achieved with liquid nitrogen (LN $_2$, 77 K) or ethanol-dry ice (EtOH-dry ice, 195 K) before undergoing purification [11, 12]. Cryogenic focusing on adsorbents is also performed before the sample is introduced into either the mass spectrometer [8, 13, 14] or the laser spectrometer [5–7]. For sample transport, adsorbent-filled dead-end cold traps are sometimes employed, in which gas samples are cryogenically trapped and sealed with gastight valves. However, the cryogenic handling of gases can induce significant isotopic fractionation if the sample is incompletely trapped or non-quantitatively released [15, 16]. To preserve the isotopic signature of methane adsorbate, adsorbents should at best:

- i. trap and release the adsorbate quantitatively,
- ii. not react and alter the adsorbate,
- iii. be easy to handle and regenerate.

These criteria are particularly important for dead-end cryotraps, such as cold fingers or containers, which cannot be purged with inert gases as is possible in chromatographic setups. Heating the cryotrap often mitigates the non-quantitative recovery of samples from such traps. While heating is a common practice in bulk isotope analysis [12, 15], its effects on temperature-sensitive clumped isotopes remain poorly studied, and excessive heating poses a risk of altering inherent clumped temperature signals by inducing isotope reordering.

This technical paper takes advantage of the rapid, high-throughput QCLAS method [7] to systematically investigate the isotope effects associated with methane desorption from silica gels, activated carbon, and zeolite molecular sieves. Target performance criteria for apparent isotope effects introduced by cryofocusing were defined as 0.1% for $\delta^{13}\text{C-CH}_4$, 1% for $\delta\text{D-CH}_4$, 0.15% for $\Delta^{13}\text{CH}_3\text{D}$, and 1.5% for $\Delta^{12}\text{CH}_2\text{D}_2$, inline with current best practices in analytics. Although QCLAS is the analytical platform used here, the results also apply to HR-IRMS.

2 | Methods & Experiments

2.1 | Adsorbents and Experimental Setup

A list of tested adsorbents is provided in Table 1. The experiments were conducted using two multi-purpose stainless-steel vacuum lines of similar design, which are schematically summarized as a single line in Figure 1 for simplicity. The vacuum lines operated at pressures below $0.1 \, \text{Pa} \, (1 \times 10^{-3} \, \text{mbar})$, achieved using either a screw pump (NeoDry7E, Kashiyama Ind., Japan) or a rotary vane pump (Rotary Vane 3, Edwards GmbH,

Germany). Pressure was monitored using a Leo 2 manometer (Keller Druckmesstechnik, Switzerland), which had a pressure range of $0-4\times10^5$ Pa (0-4 bar) with a resolution of 100 Pa and a full-scale uncertainty of 0.1%.

Methane sorption tests and transport experiments were performed with customizable stainless-steel containers ($n\!=\!15$) constructed from standard ½" Swagelok© components ($5.5\pm0.2\,\mathrm{mL}$ volume; see Supplementary information for images, item list, and order numbers). Key components of the containers included a 10-cm-long tube attached to a plug (at the bottom) and a 2- μ m filter with a vacuum-tight membrane valve (at the top), facilitating easy replacement of the adsorbent material by simply unscrewing the container body from its assembly. To ensure additional dust protection, a small loose ball of cotton and silver wool was placed on top of the adsorbent after loading.

The adsorbent materials were conditioned under continuous vacuum at temperatures ranging from 160°C to 180°C for at least 12 h. This was accomplished by connecting the containers to the vacuum line via flexible hosing and placing the container bodies into a heated aluminum block holder (Figure 1). After conditioning, the sample container valves were closed to maintain the internal vacuum.

2.2 | Testing the Maximum Methane Loading Capacity of Adsorbents

The maximum methane loading capacity of the adsorbents was tested by loading $0.50\pm0.01\,\mathrm{g}$ of adsorbent into a sample container and conditioning it as described in Section 2.1. The sample containers were then connected to valve V2 (Figure 1), and the air between V2 and the container was evacuated. Subsequently, V2 was closed while the container valve remained open. The container body was submerged in liquid nitrogen (LN₂), cooling it to the lower side of the filter, and left to equilibrate for at least 5 min before starting the adsorption test.

Methane was supplied using a volume-calibrated syringe $(Codan^*)$ equipped with a luer stopcock, filled with $5.4\,\mathrm{mL}$ of methane at standard pressure and temperature. The incremental $5.4\,\mathrm{mL}$ injections define the experimental resolution, with $0.4\,\mathrm{mL}$ stemming from the luer stopcock volume. Methane samples were drawn from a lecture bottle and the loaded syringe connected to the vacuum line at the syringe port (Figure 1). Air in the volume between the stopcocks ($<0.5\,\mathrm{mL}$) was pumped away, and the vacuum line was isolated from the pump (by closing V1) when the pressure dropped below $100\,\mathrm{Pa}$.

By opening the luer stopcock, methane gas was transferred from the syringe into the vacuum line. Then, by opening V2, the methane was directed to the cryogenic adsorbent. The vacuum pressure typically stabilized within 2 min, and a pressure reading was recorded exactly 3 min after injection to ensure comparability.

Methane injections were repeated until the adsorbent was fully saturated, as indicated by a pressure plateau near 1200 Pa

TABLE 1 | Overview of tested adsorbents.

<u> </u>						Particle	diameter		Max. CH ₄ load *
Identifier	Туре	Brand / Name	Supplier	Cat. No.	Source/ charge	mesh	mm	Pore size	ml/g
SG-1	Silica gel	Supelco TG 40	Merck	214426	MKCV9174	6/14	1.4-3.4	n/a	103
SG-2	Silica gel	TG 60	Roth	9833.1	193337745	6/16	1.0-3.0	n/a	93
SG-3	Silica gel	Supelco Davisil TG 12	Merck	214396	BCCJ4814	28/200	0.07-0.6	22 A	33
SG-4	Silica gel	Tokio Davisil TG 12	Merck	214396	BCBX1695	28/200	0.07-0.6	22 A	64
SG-5	Silica gel	High-purity grade	Merck	288594	STBL2782	200/400	0.04-0.07	60 A	21
MS3A	Molecular Sieve	Molecular sieves 3A	Merck	69832	BCBP5552V		1.6 - 5.0	3A	saturated
MS-5A	Molecular Sieve	MS-5A	Ohio Valley	5442	04Y25	100/120	0.12-0.15	5A	76
MS-13X	Molecular Sieve	Supelco MS-13X	Merck	20305	141939	60/80	0.17-0.25	10A	73
AC-1	activated carbon	Darco	Merck	242268	72096НЈ	20/40	0.4-0.8	n/a	135
AC-2	activated carbon	Extra pure	Merck	1.02514	109687	12	1.5	n/a	208

Note: n/a = not available; Cat. no. = Catalog Number; TG = Technical Grade.

(12 mbar), corresponding to the methane vapor pressure at 77 K [17]. An adsorbent was considered to begin reaching saturation when the pressure reading exceeded 100 Pa (1 mbar) 3 min after injection. This instance was defined as the *saturation point*, and the total methane volume injected was used to calculate the loading capacity in mL CH₄ per g adsorbent. This measurement had an uncertainty of approximately $\pm 2.7\,\mathrm{mL}\cdot\mathrm{g}^{-1}$ due to the 5.4 mL injection resolution.

2.3 | Testing for Isotope Effects of Methane Desorption After Cryofocusing

To study the isotope effects caused by methane storage, containers were loaded with sufficient absorbents (MS, SG, and AC) to retain 50 mL of methane. Conditioned containers were loaded with 40 mL methane on the vacuum line, which was directly connected to an in-house methane reference gas tank (EP-06, see Section 2.4 for isotopic composition) and was equipped with a sealable 10 mL volume (Figure 1) for the intermitted methane storage.

Before loading, the vacuum line plumbing and reference gas cylinder were purged multiple times with methane reference gas by opening V4 to eliminate any fractionated residuals. Following purging, the vacuum line and the 10 mL buffer volume were evacuated for over 1 min. After closing valve V1, the vacuum line and buffer volume were pressurized to 4×10^5 Pa (4 bar) with methane reference gas, allowing the gas to equilibrate for at least 1 min. Valve V3 was then closed to isolate 40 mL of methane in the 10-mL buffer volume while the remainder of the vacuum line was evacuated for at least 2min to ensure that all residual methane was removed $(p < 100 \,\mathrm{Pa})$. Subsequently, valves V2 and V3 were opened to transfer the methane into the LN2-cooled sample container, which had been cooled for a minimum of 5 min, as described in Section 2.2. During the transfer, the pressure was continuously monitored; typically, it dropped below 100 Pa within a few tens of seconds. Gas trapping lasted exactly 3 min, after which V2 and the container valve were closed.

The loaded container was then placed in a water bath at room temperature (21 ± 1 °C), and the time elapsed until the QCLAS

^aAt liquid nitrogen temperature, 77 K. Based on zero-line, see text.

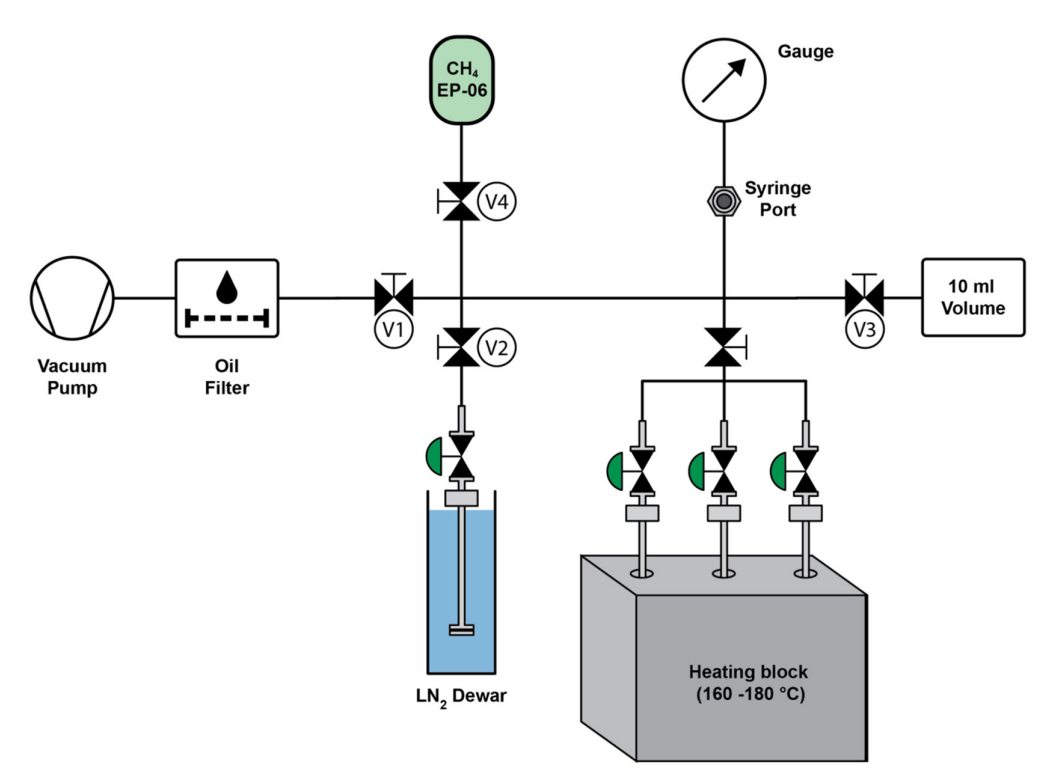


FIGURE 1 | Schematic of the two vacuum lines and experimental setups. Line 1 consisted of a rotary vane pump, oil filter, vacuum gauge, and syringe port. It was connected to the heating block and had a port for attaching storage volumes. Line 1 was used to condition the adsorbent and to perform methane loading tests. Line 2 was operated with an oil-free screw pump and was equipped with a vacuum gauge, 10 mL storage volume, and a port to connect the storage containers. Line 2 had a direct connection to the in-house methane reference gas bottle (EP-06) and was used to load the adsorbents with the methane reference gas cryogenically.

measurement was recorded. Dwelling times prior to analysis were varied between 5 and 240 min for room-temperature storage and were fixed at 5 min for experiments conducted at elevated desorption temperatures of 50 °C, 80 °C, and 95 °C (± 1 °C).

2.4 | QCLAS System and Calculation of Isotope Ratios

The methane bulk (δ D-CH₄ and δ^{13} C-CH₄) and clumped (Δ^{13} CH₃D and Δ^{12} CH₂D₂) isotopic composition were analyzed using QCLAS (Aerodyne Research Inc., USA). The spectrometer is equipped with an astigmatic Herriot-type multipass absorption cell providing 413 m optical path length with a total cell volume of 2.7 L. Two room-temperature quantum cascade laser sources (QCLs, Alpes Lasers, Switzerland) are tuned to $1077\,\mathrm{cm^{-1}}$ for analysis of 12 CH₃D and 12 CH₂D₂, and $1163\,\mathrm{cm^{-1}}$ for analysis of 12 CH₄, 13 CH₄, and 13 CH₃D. For reproducible sample injections into the multipass cell (dp/P=±0.05), the spectrometer is equipped with a high-vacuum gas inlet system operated by automated pneumatic valves and controlled by the system software (TDLWintel, Aerodyne Research Inc., USA). The spectrometer cell and gas inlet system were evacuated to < 10^{-2} Pa with a turbomolecular pump (HiCube 80 Eco, Pfeiffer Vacuum AG, Switzerland).

Each measurement cycle began with a background absorption measurement with an N₂-filled cell at 1500 Pa. Subsequently, reference and sample gases were each analyzed for 200 s at a cell pressure of 1000 Pa, with the entire analytical sequence lasting 17 min. Isotope ratios were calculated based on selected rotational lines: $^{12}\mathrm{CH_3D}$ (1076.8447 cm $^{-1}$), $^{12}\mathrm{CH_4}$ (1163.4937 cm $^{-1}$), $^{13}\mathrm{CH_4}$ (1163.6288 cm $^{-1}$), $^{13}\mathrm{CH_3D}$ (1163.4737 cm $^{-1}$), and $^{12}\mathrm{CH_2D_2}$ (1076.9698 cm $^{-1}$). Further details about the QCLAS system and analytical protocols can be found in Zhang et al. [7].

All experiments used the in-house working reference gas EP-06, a high-purity methane gas (grade 5.5, Linde Gas) with $\delta^{13}\mathrm{C_{VPDB}}\!=\!-43.75\pm0.1\%$ and $\delta\mathrm{D_{VSMOW}}\!=\!-188.7\pm2.4\%$, referenced against the University of Indiana methane standards [18] by GC-C-IRMS at the Geological Institute at ETH Zürich [19]. The clumped isotope composition of EP-06 is 3.58 \pm 0.02% for $\Delta^{13}\mathrm{CH_3D}$ and $8.90\pm0.23\%$ for $\Delta^{12}\mathrm{CH_2D_2}$, as determined with heated gases [7]. The results presented in this study were calculated as follows:

$$\delta^{13}\text{C-CH}_4 = \left(\frac{(^{13}CH_4/^{12}CH_4)_{sample}}{(^{13}CH_4/^{12}CH_4)_{reference}} - 1\right) \cdot 1000 \tag{1}$$

$$\delta \text{D-CH}_4 = \left(\frac{(^{12}CH_3D/^{12}CH_4)_{sample}}{(^{12}CH_3D/^{12}CH_4)_{reference}} - 1\right) \cdot 1000 \tag{2}$$

$$\delta^{13}CH_3D = \left(\frac{\left(^{13}CH_3D/^{12}CH_4\right)_{sample}}{\left(^{13}CH_3D/^{12}CH_4\right)_{reference}} - 1\right) \times 1000$$
 (3)

(1 s.d.) for single methane measurements, while we report one standard deviation uncertainties for replicate measurements $(n \ge 3)$.

$$\delta^{12}CH_2D_2 = \left(\frac{\left(^{12}CH_2D_2/^{12}CH_4\right)_{sample}}{\left(^{12}CH_2D_2/^{12}CH_4\right)_{reference}} - 1\right) \times 1000 \quad (4)$$

$$\Delta^{13}CH_3D = \left(\frac{\binom{13}{3}CH_3D/^{12}CH_4}{\binom{13}{3}CH_3D/^{12}CH_4}\right)_{percence} - 1\right) / \left(\left(\frac{\delta^{13}C_{VPDB}}{1000} + 1\right) \times \left(\frac{\delta D_{VSMOW}}{1000} + 1\right) - 1\right) \times 1000$$
 (5)

$$\Delta^{12}CH_2D_2 = \left(\frac{\left(^{12}CH_2D_2/^{12}CH_4\right)_{sample}}{\left(^{12}CH_2D_2/^{12}CH_4\right)_{reference}} - 1\right) / \left(\left(\frac{\delta D_{VSMOW}}{1000} + 1\right) \times \left(\frac{\delta D_{VSMOW}}{1000} + 1\right) - 1\right) \times 1000 \tag{6}$$

For the current study, the reported δ - and Δ -values are calculated as the deviation relative to the CH $_4$ reference gas EP-06. Therefore, delta values represent apparent isotope effects and should be zero within analytical uncertainties if no isotopic fractionation occurred. At time of experimentation, the external reproducibility was $\delta^{13}\text{C-CH}_4$: $\pm 0.1\%$, $\delta \text{D-CH}_4$: $\pm 1\%$, $\Delta^{13}\text{CH}_3\text{D}$: $\pm 0.15\%$, and $\Delta^{12}\text{CH}_2\text{D}_2$: $\pm 1.5\%$, which was chosen as the target performance for the cryofocusing experiments. These values are also reported as analytical uncertainties

3 | Results

3.1 | Maximum Methane Loading Capacity of Adsorbents at 77 K

Figure 2 provides an overview of the adsorbent saturation measurements. Material-specific saturation points are reported in Table 1. All tested adsorbents, except MS-3A,

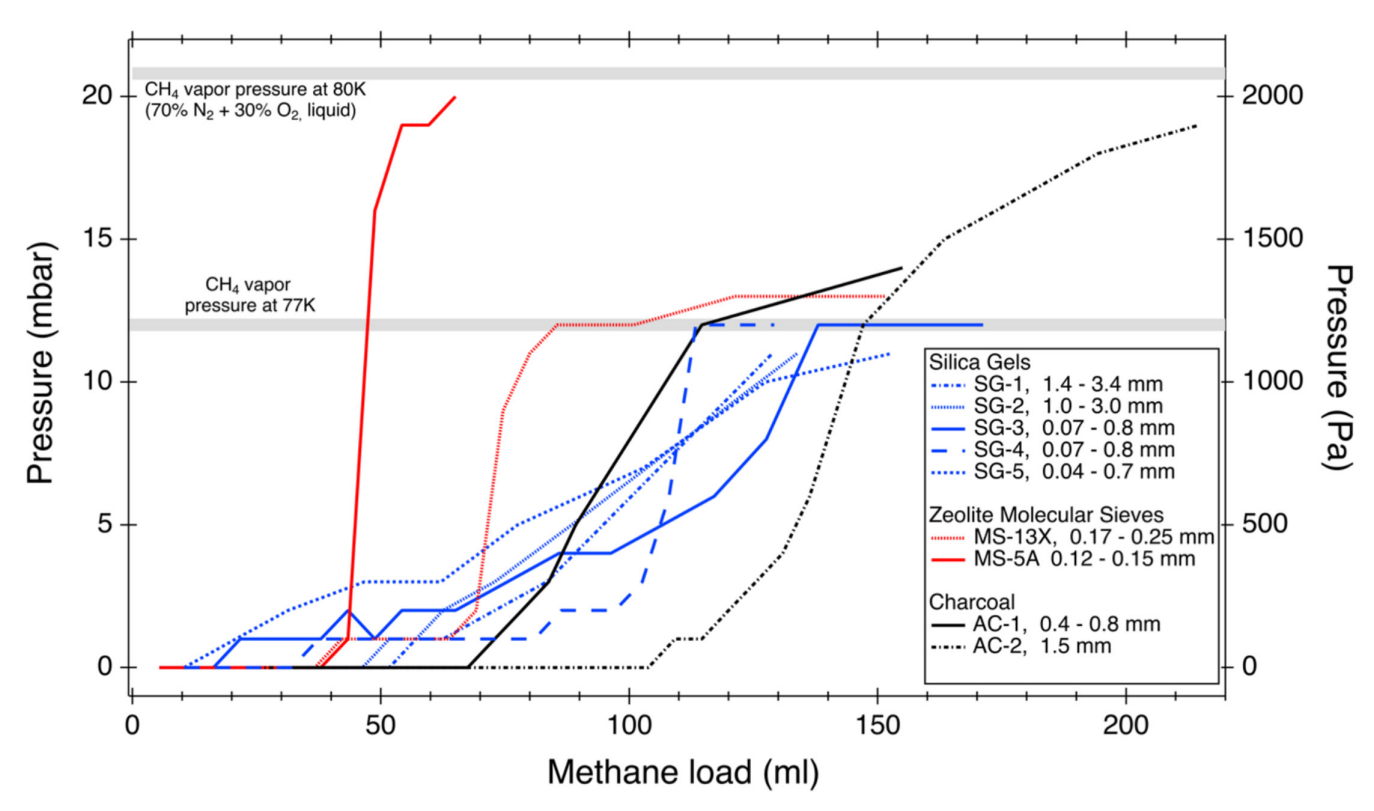


FIGURE 2 | Comparison of methane loading capacities for silica gel, molecular sieve, and charcoal adsorbents (see Table 1). Containers filled with 0.50 ± 0.01 g of adsorbent were conditioned under vacuum at $160^{\circ}\text{C}-180^{\circ}\text{C}$ for > 12h. The containers were subsequently cooled to 77 K using LN₂ while connected to a vacuum line. Methane was injected in 5 mL increments, and the pressure was monitored. Pressure readings were taken exactly 3 min after each methane injection. In most cases, methane adsorption was rapid, with baseline pressure ($< 100 \, \text{Pa}$) reached within seconds. As loading increased, methane began accumulating in the gas phase, with the onset of pressure defining the saturation point. Full saturation of the adsorbent was reached when a methane vapor pressure of 1200 Pa was achieved. The observed vapor pressure slightly exceeded 1200 Pa in a few experiments, which was attributed to a rise in the boiling point of liquid nitrogen, probably due to impurities (e.g., oxygen) condensed into the cryogen (see supplementary information). MS-3A is not shown. Its vapor pressure reached from 1200 to 2500 Pa.

demonstrated the capability to trap at least small methane volumes quantitatively ($p < 100 \, \text{Pa}$). Adsorption capacities for silica gels ranged from 21 to $103 \, \text{mL/g}$, with a positive correlation between adsorption capacity and average adsorbent grain size (Figure S1).

Among the silica gels, SG-1 (1.4–3.4 mm, $103\,\text{mL/g}$) and SG-2 (1–3 mm, $93\,\text{mL/g}$) exhibited the best adsorption performance. The worst performance was observed with the fine-powdered SG-5 (0.07–0.07 mm, $21\,\text{mL/g}$), which was excluded from subsequent testing. SG-3 was tested twice, yielding reproducible adsorption profiles and a consistent saturation point near $33\,\text{mL/g}$ (Figure S2).

Methane loading with MS-3A was unsuccessful, as vapor pressure built up immediately (1200 Pa after an initial 10 mL injection; Figure S3). This outcome can be attributed to the similar pore size of MS-3A and the kinetic diameter of methane (3.6 Å vs. 3.8 Å), which saturates the zeolite surface and leaves minimal opportunity for methane molecules to penetrate the zeolite structure [15]. Consequently, MS-3A was excluded from further testing. The saturation points for MS-5A and MS-13X were nearly identical, at 76 and 73 mL/g, respectively. However, their adsorption profiles differed after saturation. While MS-5A was quickly saturated with a corresponding buildup of methane vapor pressure, MS-13X maintained low methane vapor pressure until a sudden full saturation occurred near 160 mL/g (Figure 2).

The highest adsorption capacities were observed for adsorbents made of activated charcoal, AC-1 (135 mL/g) and AC-2 (208 mL/g). For both AC adsorbents, the pressure buildup was gradual, approaching a maximum load of approximately 300 and 400 mL/g, respectively, when reaching the vapor pressure. In a few experiments, an increase in the CH₄ vapor pressure above 12 mbar was observed (e.g., MS-5A, AC-2). This was attributed to an increase in the boiling point due to the evaporative enrichment of oxygen impurities in the cryogen (cf. Supplementary information [20]). Quantitative cryogenic trapping of methane was not feasible with non-loaded, i.e., adsorbent-free, containers, as the methane vapor pressure over ice at 77 K is approximately 12 mbar [17].

3.2 | Isotope Effects of CH₄ Cryofocusing

Two experiments were conducted to evaluate isotope fractionation after cryogenic trapping.

- Desorption or dwell time-series experiments (Section 3.2.1):
 Desorption time-series experiments were performed at 21±1°C to determine the minimum time required for the headspace gas to reach isotopic equilibrium between adsorbed and gas-phase CH₄ (Figure 3). The underlying assumption is that desorption and the diffusive escape of methane from the porous adsorbent would result in kinetic isotope fractionation.
- 2. Temperature-dependent desorption experiments (Section 3.2.2): A second experiment examined isotope effects apparent after methane desorption at varying temperatures while maintaining a constant desorption

time (Figure 4). This test explored whether heating the container could reduce desorption time and whether heating skews clumped isotope values.

The performance targets for isotopic precision listed in Section 2.4 were used to interpret the apparent isotope effects:

- 1. **Good/Best Performance:** The absolute value of the apparent isotope effect is within the performance target, and its standard deviation for repeated analyses overlaps with zero. Hence, the absolute value is indistinguishable from the reference gas value.
- 2. **Satisfying Performance:** The absolute value of the apparent isotope effect is within performance targets, but its standard deviation does not overlap with zero.
- 3. **Moderate Performance:** The absolute value of the apparent isotope effect is outside the performance target, but its standard deviation overlaps with it.
- 4. **Poor Performance:** The absolute value of the apparent isotope effect is outside the performance target, and its standard deviation for repeated analyses does not overlap with zero.

The most relevant results are summarized in Table 2 and Figure 5.

3.2.1 | Desorption or Dwell Time Series Experiments

Desorption time-series experiments were conducted at room temperature ($21\pm1^{\circ}$ C), except for SG-4, where experiments were performed at both $21\pm1^{\circ}$ C and $50\pm1^{\circ}$ C. Among the silica gels, the three best-performing adsorbents in terms of adsorption capacity, SG-1, SG-2, and SG-4, were tested. Additionally, MS-5A, MS-13X, AC-1, and AC-2 were included in the experiments.

<u>Carbon Isotopes.</u> Fractionation in δ^{13} C-CH₄ of up to 3.5% was observed for the shortest desorption runtimes (Figure 3A), regardless of adsorbent type. Methane desorbed from SG-1 and SG-2 showed initial δ^{13} C depletion but leveled off within the performance target after 120-150 min. After dwell times exceeding 120 min, SG-1 and SG-2 yielded −0.04 ± 0.06‰ and $-0.14 \pm 0.04\%$, respectively. Methane desorbed from SG-4 (both 21°C and 50°C series) showed up to 3.5% enrichment in δ^{13} C-CH₄ for the shortest dwelling times but reached the performance target after 150 min $(0.14 \pm 0.09\%)$ at 21°C and $0.11 \pm 0.04\%$ at 50°C). MS-5A experiments with dwell times between 110 and 170 min at 21°C produced δ^{13} C-CH₄ values indistinguishable from zero $(-0.01 \pm 0.09\%)$. Methane freshly desorbed from MS-13X adsorbent exhibited enrichment up to 3.4% in ¹³C/¹²C, displaying apparent isotope effects of 0.3%-0.9% even after more than 130 min of dwell time. No MS-13X experiments reached the performance target. Methane desorbed from AC-1 exhibits 3.5% enrichment in ¹³C/¹²C after a 25-min dwell time. Values approached the performance target after 190 min (0.19 \pm 0.13%), but on average, a fractionation of $0.4 \pm 0.2\%$ was observed for longer experiments (>200 min). AC-2 consistently showed moderate performance for δ^{13} C, with most samples exceeding

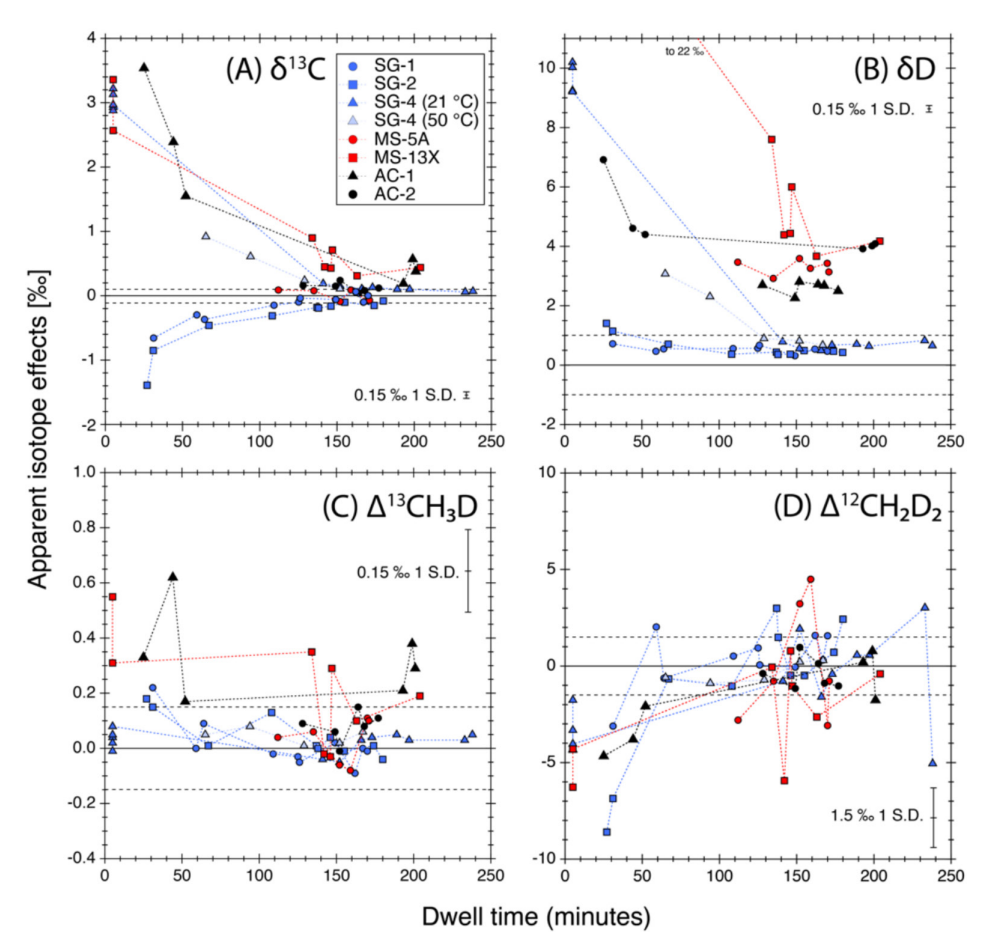


FIGURE 3 | Desorption time-series experiments. Containers loaded with 40 mL of methane (t=0 min) were warmed in a water bath to room temperature (21°C; one experiment at 50°C) for up to 240 min before isotope measurement using the QCLAS system. For short dwell times, all adsorbents exhibited deviations from zero due to insufficient desorption, with the most pronounced effects observed in δ^{13} C and δD . Isotope fractionation diminished for most materials after dwelling for > 120 min at room temperature. Δ^{12} CH₂D₂ equilibrated within 60 min, while Δ^{13} CH₃D was the least affected by insufficient dwelling time. Silica gels (blue symbols) demonstrated the best overall performance, showing high reproducibility across all isotopologues and a consistent +0.5‰ enrichment in δD . Molecular sieves and charcoals provided adequate performance for clumped isotopes but introduced significant fractionations in δ^{13} C (up to +0.5‰) and δD (up to +4‰). A desorption time-series experiment at 50°C for SG-4 showed no improvement in reducing the minimum dwell time for this particular adsorbent. Dashed lines represent performance target.

120 min, yielding values around $0.13\pm0.07\%$. It remains to be tested whether the $^{13}\text{C}/^{12}\text{C}$ ratio increases when dwell time exceeds 200 min. Adsorbent-free cylinders reproduced the reference gas value within uncertainty $(0.08\pm0.17\%)$. Overall, SG-1 and MS-5A yield the best adsorbent performance at room temperature and > 120 min of dwelling time.

Hydrogen Isotopes. All adsorbent materials caused fractionation in δ D-CH₄, ranging from +0.4‰ to +10‰, even for extended dwell times. This fractionation is no experimental or analytical artifact, as methane frozen into empty containers yielded nearzero δ D-values of 0.07±0.02‰ (n=7). SG-1 and SG-2 reached the performance target after ~60 min and yielded reproducible results after more than 120 min (0.52±0.12‰ and 0.42±0.05‰, respectively). Methane desorbed from SG-4 showed initial fractionation of up to +10‰, stabilizing at 0.80±0.11‰ for 21°C and 0.67±0.11‰ for 50°C after more than 120 min. Generally, all silica gels exhibited fractionation near +0.5‰.

Zeolite molecular sieves and charcoal showed larger D/H fractionations. Methane desorbing from MS-13X was enriched

in D by up to 22% for dwell times of around 5 min, stabilizing at $4.6\pm1.2\%$ after more than 120 min. MS-5A displayed a similar, but more reproducible, fractionation at $3.3\pm0.2\%$ for dwell times exceeding 110 min. Charcoal adsorbents exhibited fractionations of $4.0\pm0.1\%$ for AC-1 and $2.7\pm0.1\%$ for AC-2. Adsorbent-free cylinders maintained the isotopic composition of the reference gas satisfactorily $(0.07\pm0.02\%)$.

For analyzing methane bulk hydrogen isotope composition from cryosorbed samples, silica gels outperformed zeolite molecular sieves and activated carbon, with SG-1 and SG-2 delivering the best results.

<u>Clumped Isotope</u> Δ^{13} <u>CH</u>₃<u>D</u>. Most Δ^{13} CH₃D values for CH₄ desorbed from silica gels fell within the performance target of $\pm 0.15\%$, with no significant trends observed. For dwell times exceeding 120 min, values were indistinguishable from zero, i.e., SG-1= $-0.03\pm0.04\%$, SG-2= $0.00\pm0.03\%$, SG-4 (21°C)= $0.03\pm0.03\%$, and SG-4 (50°C)= $0.04\pm0.04\%$. Among zeolites, MS-5A yielded values indistinguishable from zero ($0.04\pm0.08\%$), while MS-13X showed larger deviations. For

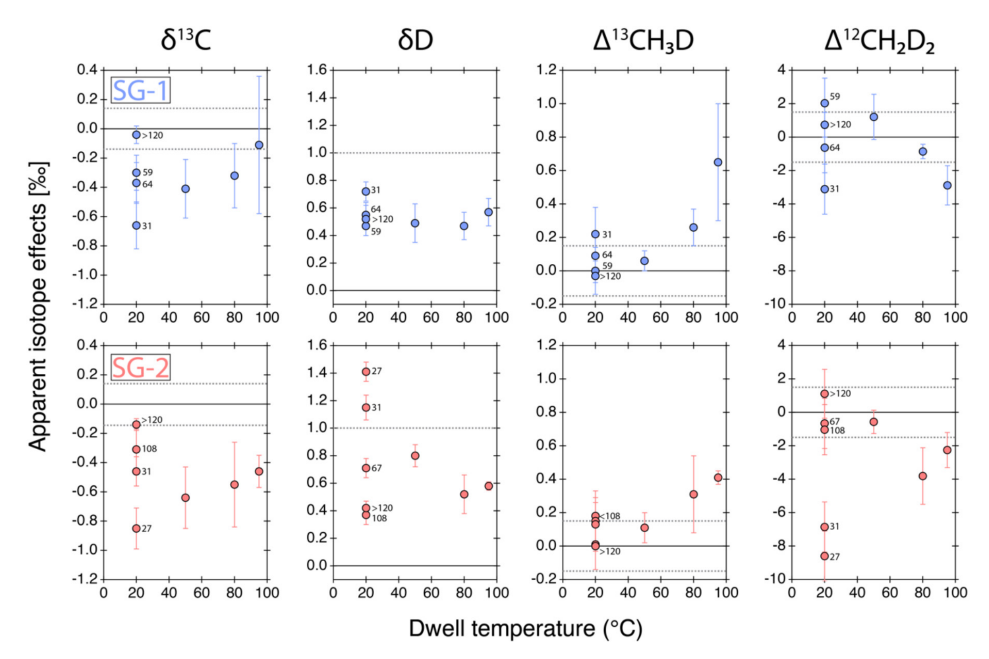


FIGURE 4 | Effect of heating silica gel traps on methane desorption before measurement (SG-1: blue symbols; SG-2: red symbols). Dashed lines indicate the tolerance band for acceptable values. Numerical annotations represent dwelling times in minutes at room temperature. Unannotated data points correspond to samples that dwelled for 5 min in a heated water bath. The 5- and > 120-min data points are averages of multiple measurements ($n \ge 3$), while other data points represent single measurements. Higher desorption temperatures facilitated equilibration for bulk carbon isotopes (δ¹³C), with 95°C samples achieving values closer to zero than lower temperature samples. For δD, desorption temperature had minimal impact, except for SG-2 desorbed at 21°C, which required approximately 60 min to reach accepted values. Short dwelling times at 80°C and 95°C significantly skewed Δ 3CH₂D₂ values, whereas dwelling at 50°C for 5 min retained Δ -values at acceptable level. For room temperature desorption (21°C), a minimum of 60 min of dwelling time is recommended for both SG-1 and SG-2.

MS-13X, 5-min dwell times resulted in $\Delta^{13}\text{CH}_3\text{D}$ values up to 0.6‰, remaining slightly elevated for dwell times longer than 120 min (0.19 ± 0.09‰). Charcoal adsorbents displayed variable performance. Methane desorbed from AC-1 consistently exhibited elevated $\Delta^{13}\text{CH}_3\text{D}$ values (0.29 ± 0.08‰ for dwell times > 120 min). In contrast, AC-2 achieved satisfactory performance, with values near zero (0.08 ± 0.07‰ for dwell times > 120 min). Adsorbent-free cylinders reproduced the reference gas value within uncertainty (0.05 ± 0.12‰).

Overall, the silica gels provided the best adsorbent performance, with $\Delta^{13} \text{CH}_3 \text{D}$ values indistinguishable from the reference gas within uncertainty.

<u>Clumped Isotope</u> $\Delta^{12}CH_2D_2$. Methane desorbed from all adsorbent materials showed apparent isotope effects up to −9‰ for dwelling times shorter than 60 min. However, silica gels dwelling for more than 120 min reproduced the reference gas value within uncertainty, i.e., $SG-1 = -0.74 \pm 0.74\%$, $SG-2 = 1.11 \pm 1.45\%$, SG-4 (21°C) = $0.06 \pm 0.56\%$, and SG-4 (50°C) = $-0.22 \pm 2.45\%$). CH₄ desorbed from MS-13X was fractionated at shorter dwell times (-4% to -6%) but achieved the performance target after dwell times exceeding 120 min (-1.4 ± 1.2%). MS-5A met the performance targets but with a relatively large uncertainty $(0.05 \pm 2.86\%)$. Both AC-1 and AC-2 provide apparent isotope effects within performance targets after dwell times > 120 min (AC-1: $-0.26 \pm 1.33\%$, AC-2: $-0.4 \pm 0.8\%$). Adsorbent-free cylinders reproduced the reference gas value within uncertainty $(0.89 \pm 0.89\%)$. Overall, silica gels, MS-5A, and activated carbon demonstrated good adsorbent performance for Δ12CH2D2, with

silica gels (notably SG-4 at room temperature) reproducing the reference gas value best and at the lowest uncertainties.

3.2.2 | Heated Desorption Experiments

Figure 4 presents the results of heated desorption experiments performed at 21°C, 50°C, 80°C, and 95°C using SG-1 and SG-2. Additional results for other silica gels, zeolite molecular sieves, and charcoal adsorbents are shown in Figure 5. SG-1 and SG-2 were examined in greater detail due to their superior performance in the time-series experiments (Section 3.2.1). For experiments conducted at 50°C–95°C, the adsorbent was heated in a water bath for 5 min prior to measurement. The time-series experiments performed at 21°C (Section 3.2.1) are shown for comparison. Results for dwell times exceeding 120 min were averaged.

Carbon Isotopes. Heating generally reduced fractionation in δ^{13} C. For SG-1 at 95°C, the performance target was nearly met, albeit with a relatively large uncertainty ($-0.11\pm0.47\%$). All other SG-1 and SG-2 experiments at 21°C-95°C with dwell times under 120 min did not meet the performance target. Achieving satisfactory performance for δ^{13} C-CH₄ required at least 120 min of dwelling at 21°C. The best performance was observed for MS-5A at 21°C and 80°C, as well as for AC-2 at 80°C, both showing apparent isotope effects outside performance targets but within uncertainties (standard deviation for repeated experiments). Large fractionations between 0.4‰ and 1.5‰ were observed for MS-13X and AC-1.

TABLE 2 | Summary of desorption experiments—For performance evaluation see text.

Series	8	δ ¹³ C			δD		Δ^{13} CH ₃ D	H ₃ D		Δ ¹² C	Δ^{12} CH ₂ D ₂		<i>δ</i> ¹³ C	δ^{13} CH ₃ D		<i>8</i> ¹² C	δ^{12} CH ₂ D ₂		NoE
Empty	0.08	+1	0.17	0.07	+1	0.02	0.05	+1	0.12	0.89	+1	0.89	0.16	+1	0.19	1.04	+1	06.0	7
SG-1 - 95 °C	0.11	+I	0.38	0.57	+1	0.10	0.65	+1	0.35	-2.88	+1	1.17	0.87	+1	0.75	-1.75	+I	1.29	3
SG-1 - 80 °C	-0.29	+I	0.23	0.43	+1	0.05	0.23	+1	0.07	-0.86	+1	0.43	0.25	+I	0.24	0.01	+1	0.51	5
SG-1 - 50 °C	-0.41	+I	0.20	0.49	+1	0.14	90.0	+1	90.0	1.21	+1	1.35	0.00	+1	0.31	2.20	+I	1.41	9
SG-1 - 22 °C	-0.04	+I	90.0	0.52	+1	0.12	-0.03	+1	0.04	0.74	+1	0.74	0.29	+1	0.12	1.77	+I	0.79	9
SG-2 - 95 °C	-0.46	+I	0.11	0.62	+1	0.09	0.35	+1	0.13	-2.25	+1	1.05	0.38	+ I	0.16	-1.01	+I	1.12	5
SG-2 - 80 °C	-0.55	+I	0.29	0.52	+1	0.14	0.31	+1	0.23	-3.81	+1	1.69	0.08	+1	0.13	-2.78	+I	1.78	9
SG-2 - 50 °C	-0.64	+I	0.21	08.0	+1	0.08	0.11	+1	60.0	-0.57	+1	0.70	0.20	+1	0.20	1.04	+ I	0.65	5
SG-2 - 21 °C	-0.14	+I	0.04	0.42	+1	0.05	0.00	+1	0.03	1.11	+1	1.46	0.08	+ I	0.07	1.96	+ I	1.46	9
SG-3 - 80 °C	0.18	+I	0.26	1.06	+1	0.41	0.05	+1	0.04	-0.31	+1	1.75	1.18	+ I	89.0	1.81	+I	2.44	5
SG-4 - 50 °C	0.11	+1	0.04	0.67	+1	0.11	0.02	+1	0.04	-0.22	+1	2.45	99.0	+1	0.08	1.12	+I	2.52	8
SG-4 - 22 °C	0.14	+I	0.09	08.0	+1	0.11	0.03	+1	0.03	-0.06	+1	0.56	0.70	+ I	0.20	1.54	+ I	0.40	3
MS-5A - 80 °C	-0.05	+I	0.12	3.36	+1	1.01	0.13	+1	80.0	0.16	+1	1.83	3.36	+I	1.04	88.9	+1	2.15	∞
MS-5A - 22 °C	-0.01	+I	0.09	3.29	+1	0.23	0.04	+1	80.0	0.05	+1	2.86	3.08	+1	0.14	6.64	+I	2.96	7
MS-13X - 80 °C	1.50	+I	0.97	9.65	+1	5.94	0.30	+1	60.0	-2.78	+1	3.12	11.26	+1	7.05	16.57	+I	9.04	9
MS-13X - 22 °C	0.54	+I	0.22	5.05	+1	1.47	0.15	+1	0.16	-1.55	+1	2.44	5.45	+I	1.90	8.56	+1	4.46	9
AC-1 - 80 °C	1.14	+I	0.70	3.54	+1	0.58	0.46	+1	0.44	-1.62	+1	0.82	4.90	+I	1.40	5.46	+1	0.82	6
AC-1 - 22 °C	0.38	+1	0.19	4.01	+1	0.09	0.29	+1	80.0	-0.26	+1	1.33	4.69	+1	0.34	7.78	+1	1.23	3
AC-2 - 80 °C	-0.10	+1	0.25	1.65	+1	0.29	0.68	+1	0.28	-3.03	+1	1.23	2.05	+1	0.38	0.26	+1	1.31	10
AC-2 - 22 °C	0.13	+1	0.07	2.61	+1	0.20	0.08	+1	0.05	-0.40	+1	0.82	2.60	+1	0.23	4.83	+1	1.17	9
Acceptance band	0+1	± 0.1 ‰		+1	± 1.0 %		+ 0.15 %	0%		+1.	± 1.5 %		+ 0	± 0.1 %		+ 0.	0.85 %		
Dark Green: Good performance	rformance																		
Bright Green: Satisfying performance	ing perforn	nance																	
Yellow: Moderate performance	formance																		

NoE: Number of Experiments

Red: Poor performance

10970231, 2023, 13, Downloaded from https://analyticalscience/journals.onlinelibrary.wiley.com/do/io/1.002/rem.1040 by Physikalisch Tec Bundesanstalt, Wiley Online Library on 127/11/2025, See the Terms and Conditions (https://onlinelibrary.wikey.com/emms-and-conditions) on Wiley Online Library for rules of use; O. Anticles as governed by the applicable Creative Commons License

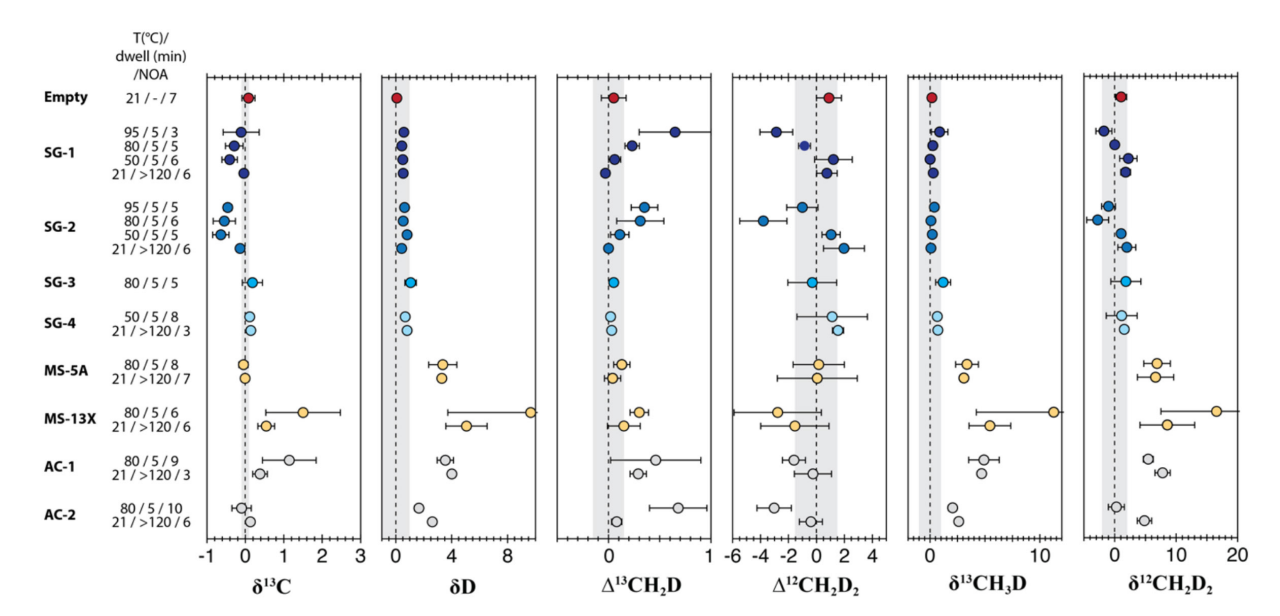


FIGURE 5 | Graphical summary of the desorption experiments. NOA = number of analyses.

<u>Hydrogen Isotopes.</u> For SG-1 and SG-2, almost all δD -CH4-values were reproduced satisfactorily across all tested temperatures (Figure 4). Heated experiments displayed consistent δD -CH $_4$ fractionation of approximately +0.5%. For SG-4, heating for 5 min at 50°C and dwelling for over 120 min at 21°C produced comparable results (0.7 \pm 0.1% and 0.8 \pm 0.1%, respectively). Heating did not mitigate the large δD -CH $_4$ fractionations observed for zeolite molecular sieves and activated carbon.

Doubly Substituted Isotopologues $\delta^{13}CH_2D$ and $\delta^{12}CH_2D_2$. Methane desorbed from silica gels showed enrichment in ¹³CH₃D by up to 1.2.%, with an average fractionation of $0.4\pm0.4\%$. The desorption temperature had no apparent effect on $\delta^{13}CH_2D$. For SG-2, dwell times exceeding 120 min at room temperature produced the most reproducible $\delta^{13}CH_3D$ values near zero. No systematic trend was observed for $\delta^{12}CH_2D_2$, with values ranging from -2.8 to +2.2‰. On average, methane desorbed from silica gels was indistinguishable from the applied reference gas $(0.5 \pm 1.7\%)$. The smallest change in $\delta^{12}CH_2D_2$ was observed for methane desorbed from SG-1 for $5 \min (0.01 \pm 0.51\%)$. Zeolite molecular sieves showed large positive fractionations, ranging from 3.1% to 11.3% for δ^{13} CH₃D and 6.6 to 16.6% for δ^{12} CH₂D₃. Methane desorbed from charcoal adsorbents was also fractionated with values up to 7.8%. Only methane desorbed from AC-2 at 80°C for 5 min yielded a δ^{12} CH₂D₂ value (0.26 ± 1.31%) within performance targets.

Clumped Isotope $\Delta^{13}\text{CH}_3D$. Heating silica gels increased $\Delta^{13}\text{CH}_3D$. Methane desorption at 80°C and 95°C from SG-1 and SG-2 resulted in up to 0.6% higher $\Delta^{13}\text{CH}_3D$ values (Figure 4). However, 5 min of dwelling at 50°C and over 120 min at 21°C produced results indistinguishable from zero within uncertainty for SG-1, SG-2, and SG-4. MS-5A reproduced the reference $\Delta^{13}\text{CH}_3D$ value at 21°C (0.04 \pm 0.08%) and showed satisfying performance at 80°C (0.13 \pm 0.08%, respectively). Among charcoal adsorbents, only AC-2 at 21°C reached target performance (0.08 \pm 0.05%).

<u>Clumped Isotope</u> Δ^{12} <u>CH</u>₂<u>D</u>₂. Methane desorbed at 80°C and 95°C from SG-1 and SG-2 exhibited slightly decreased Δ^{12} CH₂D₂

values (Figure 4). Heating silica gels for 5 min at 50°C or dwelling for 60 min at room temperature reproduced the isotopic composition of the applied reference gas within uncertainty.

MS-5A reproduced the reference gas $\Delta^{12} \text{CH}_2 D_2$ at 80°C and 21°C, but with a poorer reproducibility (0.16±1.83‰ and 0.05±2.86‰, respectively). CH₄ desorbed from MS-13X retained the $\Delta^{12} \text{CH}_2 D_2$ of the reference gas at dwell temperatures of 80°C and 21°C but with large uncertainties (–2.8±3.1‰ and –1.6±2.4‰). Both AC-1 and AC-2 showed good reproducibility at 21°C with dwell times exceeding 120 min, but heating at 80°C led to larger fractionation (1.6‰–3‰).

3.2.3 | Methane Cryotrapping Without Adsorbent

As a reference, seven experiments were conducted in which 40 mL of reference gas was frozen at 77 K into empty containers. Since the direct freezing of methane results in approximately 12 mbar vapor pressure, the trapping process is not quantitative, leading to the inevitable loss of a small fraction of gas, depending on the volume of the container. This fraction is relatively minor for the selected experimental design, as discussed in Section 4.4. The overall performance of the direct-trapping method was found to be satisfactory, with the following results: $\delta^{13}\text{C-CH}_4 = 0.08 \pm 0.17\%, \qquad \delta\text{D-CH}_4 = 0.07 \pm 0.02\%, \\ \Delta^{13}\text{CH}_3\text{D} = 0.05 \pm 0.12\%, \qquad \Delta^{12}\text{CH}_2\text{D}_2 = 0.89 \pm 0.89\%, \\ \delta^{13}\text{CH}_3\text{D} = 0.16 \pm 0.19\%, \text{ and } \delta^{12}\text{CH}_2\text{D}_2 = 1.04 \pm 0.90\%.$

4 | Discussion

4.1 | Isotopologue Alterations of Methane Desorbed From Silica Gel, Zeolite Molecular Sieves, and Charcoal

The ability of silica gels, zeolite molecular sieves, and activated carbon to preserve the isotopic signature of a $\mathrm{CH_4}$ sample varies significantly. While silica gels generally maintain the isotopic

characteristics within acceptable thresholds, methane desorbed from activated carbon and zeolite molecular sieves often exhibit substantial isotopic fractionation (Figure 5). These fractionations may result from (i) chromatographic isotope effects, (ii) chemical reactions, including reordering, on catalytic adsorbent surfaces, or a combination of both.

The chromatographic separation of isotopologues is an intrinsic property of all adsorbent materials. Heavier isotopologues typically elute first due to their smaller molecular radius [21]. This phenomenon explains the elevated $\delta\text{-values}$ observed in short-dwelling experiments (Figure 3). The duration required for complete diffusive equilibration of methane isotopologues between the pore and headspace depends on the adsorbent material, its conditioning state, and any structural blockages caused by the adsorbent or contaminants. Despite these dependencies, an apparent variability in equilibration times could not be resolved among the tested materials. Full isotopic equilibration of headspace gas at 21°C occurred after approximately 120 min (Figure 3).

Chemical alterations of methane isotopes are supported by offsets in $\delta D\text{-CH}_4$ observed across all adsorbent materials, ranging from +0.5% for silica gels to +4.6% for molecular sieves and activated carbon. Similar systematic $\delta D\text{-CH}_4$ fractionations of +0.5% have been reported for methane desorbed from MS-5A [16]. These hydrogen isotope fractionations, which were reproducible in time-series experiments, were effectively absent in adsorbent-free experiments $(0.07\pm0.02\%)$.

These alterations may arise from methane decomposition reactions that kinetically enrich heavier isotopologues [22] or hydrogen exchange reactions with functional groups on the adsorbent surface or volatile contaminants. Problematically, the activation of the methane C-H bond is energy intensive (~430 kJ/mol for direct dissociation [23]) and a measurable hydrogen exchange would be unexpected. However, zeolite molecular sieves are well-established catalysts for hydrocarbon cracking, involving hydrogen exchange via Brønsted acid groups on the zeolite pore surface [24-26]. The activation energy for C-H bond dissociation on Brønsted sites (Al-OH-Si type) is significantly reduced to ~130 kJ/mol [26]. Still, experimental D/H exchange between methane and MS-13X required elevated temperatures (> 420°C), with reaction rates decreasing to $\sim 1^{-22} s^{-1}$ when extrapolated to 21°C [24]. These findings highlight the potential for isotopologue alteration when zeolites are excessively heated during methane desorption (e.g., by torching). A positive correlation between the Al/Si ratio and exchange kinetics [24, 26] further suggests that high-Al₂O₃ domains in zeolite structures may induce isotopologue reordering. Indeed, γ-Al₂O₃ has been shown to reorder methane isotopologues and facilitate hydrogen exchange between methane and hydrogen gas at temperatures as low as 1°C over hours to days [13, 27]. It is possible that high-Al₂O₂ domains in the zeolite structure can indeed cause reordering. The importance of structural Al₂O₃ for isotopologue reordering indirectly explains the near-ideal performance of silica gels, showing limited δD alteration of the methane. Silica gels only contain trace amounts of Al₂O₃ and other contaminants, and silanol terminations are non-active for D/H exchange at such low temperatures [24, 26].

The variable performance of charcoal can be explained similarly to that of zeolite molecular sieves. Activated carbon, derived from natural precursors, often contains elevated concentrations of metals and metal oxides known to catalyze D/H exchange reactions involving methane [28]. Further, activated carbon also contains Brønsted acid sites, such as carboxylic or phenolic terminations, that can facilitate D/H exchange with contaminants or the catalyst surface.

Catalytic effects on the isotopic composition of adsorbates are most evident in hydrogen isotopes, given the relatively large fractionations commonly observed in the hydrogen system. However, other isotope systems can also be affected. For example, Meier-Augenstein et al. [29] reported alterations in carbon and oxygen isotope values in human breath samples that were dehumidified using MS-4A and MS-5A. Similarly, Stolper et al. [16] observed fractionations of up to +1.4% for δ^{13} C and δD and +0.5% for mass-18 isotopologues in methane desorbed from MS-5A. Under hydrothermal conditions, oxygen isotopes in zeolite-water systems have been shown to fully exchange within hours to days [30]. Isotope exchange between multiple volatile species retained in molecular sieves has also been reported [15].

4.2 | The Role of Adsorbent (Re-) Conditioning

To minimize efforts in regenerating adsorbents during daily analytical routines and improve efficiency, it is desirable to use adsorbents that can be easily regenerated. For this reason, we tested all adsorbent materials using a uniform, straightforward protocol: heating the adsorbents to $160^{\circ}\text{C}-180^{\circ}\text{C}$ for at least 12 h (overnight) under a dynamic vacuum of 10^{-3} mbar.

In general, desorption and reactivation of adsorbent materials at ambient pressure typically require temperatures of 120°C-200°C for silica gels [11, 12, 31] and 250°C-500°C for molecular sieves [15, 32]. For activated carbon, volatile removal generally occurs around 200°C, but completely eliminating more refractory contaminants (e.g., heavy hydrocarbons or chemisorbed hydrogen) necessitates temperatures exceeding 500°C [33]. Although operating under a vacuum can significantly reduce these activation and regeneration temperatures, the relatively mild conditioning protocol used in this study likely contributed to the observed performance discrepancies. Specifically, our heating protocol at 160°C-180°C under vacuum for more than 12h may have been insufficient to remove contaminants or residual methane completely from coals and zeolites. These residuals could facilitate D/H exchange on catalytic sites. While higher activation temperatures might have improved the performance of these materials, they would also significantly complicate the reconditioning process for the storage containers.

As discussed in Section 4.1, silica gels outperform activated carbon and zeolite molecular sieves in preserving the isotopic integrity of methane samples (Figure 5). In addition to their superior isotopic fidelity, silica gels offer practical advantages for daily laboratory use due to their relatively high adsorption capacity and consistent reproducibility of methane isotopic values. These characteristics make silica gels the ideal choice for applications in dead-end traps.

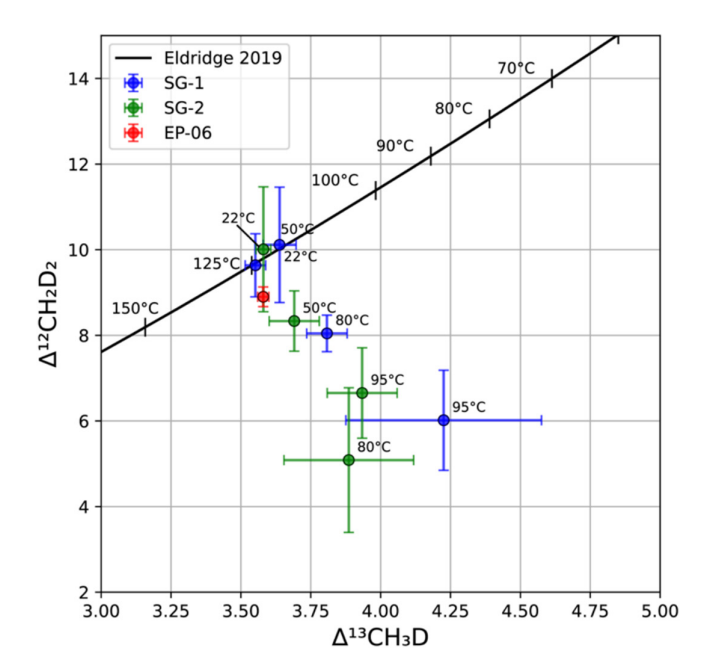


FIGURE 6 | Dual clumped isotope plot. The red symbol represents the clumped isotopic composition of EP-06, i.e., the reference gas used in the sorption experiments. Blue and green symbols correspond to results for desorption experiments conducted at 21°C to 95°C for SG-1 and SG-2, respectively. A systematic change in clumped isotopic composition with respect to EP-06 is observed at higher desorption temperatures (i.e., 80°C and 95°C). For $T \ge 50$ °C, dwell times were limited to 5 min, while experiments at 21°C dwelled for at least 120 min. Error bars are 1 s.d.

4.3 | Heating Traps for Methane Desorption

One of the main challenges of dead-end cryotraps is the potential for stagnating gas in the adsorbent, leading to incomplete sample recovery, often addressed by heating the traps. While bulk isotope ratios are generally less affected, the impact of trap heating on temperature-sensitive clumped isotope signals in methane remains unclear.

Our heating experiments on silica gel traps provide some preliminary insights. Heating SG-1 and SG-2 at 80°C and 95°C for 5 min prior to measurement resulted in systematically offset $\Delta\text{-values}$ (Figure 6). The absolute $\Delta\text{-values}$ for our EP-06 reference gas yield clumping temperatures of $\Delta^{13}\text{CH}_3D=125^\circ\text{C}$ and $\Delta^{12}\text{CH}_2D_2=137^\circ\text{C}$. The $\Delta\text{-values}$ of heated experiments deviate consistently from the equilibrium line in dual-clumped isotope space (Figure 6). These deviations may be due to reordering and isotope exchange processes.

The δD results of the time series experiments suggest that the methane isotope composition may be slightly altered, with elevated temperatures potentially enhancing catalytic exchange reactions. Alternatively, a chromatographic isotope effect cannot be excluded, as 5 min of heating duration may have been too short for complete desorption and headspace equilibration.

The increased $\Delta^{13}\text{CH}_3\text{D}$ values observed in heated experiments align with the possibility of low-temperature reordering. However, the corresponding decrease in $\Delta^{12}\text{CH}_2\text{D}_2$ is

contradictory to this interpretation. Dwelling-time experiments conducted at 21°C suggest that insufficient desorption times can also result in elevated $\Delta^{13}\mathrm{CH_3D}$ and lower $\Delta^{12}\mathrm{CH_2D_2}$ values (Figure 3C,D). On the other hand, our findings indicate that heating SG-1 at 50°C for 5 min is already sufficient to reproduce reference gas values within uncertainty, while SG-2 remains clearly offset. Notably, Sivan et al. [11] heated silica gels in a water bath at 70°C and obtained reproducible clumped values. Thus, some silica gels may be suitable for short-term moderate heating, but their application must be thoroughly tested. Notably, heating samples above 80°C may tamper with the methane clumped isotope signature. Nevertheless, these inconclusive results highlight the need for further testing and the necessity of avoiding heating at temperatures above 50°C.

The best results for all isotope ratios were obtained when desorption was allowed to proceed for at least 120 min in a water bath at 21°C. This finding is convenient, as samples in containers are typically exposed to room temperatures during handling, eliminating the need for elaborate sample-heating systems. However, caution is advised when freshly transferring a sample to a silica gel trap before an analytical session, as incomplete equilibration could still occur.

4.4 | When Should Adsorbent Materials Be Used for Methane Trapping?

There is no perfect adsorbent, and our experimental results indicate that adsorbent-free trapping may be preferable under certain circumstances for methane clumped isotope analysis. The key question is, when are adsorbent materials necessary for such analyses?

The direct freezing of methane without an adsorbent results in a temperature-dependent headspace vapor pressure, leading to potential gas loss during subsequent sample processing. For example, consider cryoloading methane in an adsorbent-free container on a vacuum line such as shown in Figure 1. The cryoloading proceeds at 77 K, resulting in a constant vapor pressure of 11.75 mbar, while the rest of the vacuum line is at room temperature. The effective amount of methane that can be trapped as ice depends here on the overall headspace volume of the vacuum line; the larger the vacuum line volume, the less methane is trapped as ice in the container. This relationship is illustrated in the contour plot in Figure 7 (details provided in the supplementary information), which shows that, at a constant methane amount, increasing headspace volume results in a higher molar vapor fraction. Similarly, increasing the methane amount will reduce the molar vapor fraction at constant headspace volume. The checkered area in Figure 7 represents the approximate range of our vacuum line volumes and the typical methane quantities handled (10-40 mL).

Methane isotopologues fractionate between the ice and vapor phase, resulting in a vapor pressure isotope effect (VPIE). Deuterated methane molecules exhibit a normal VPIE, where the vapor pressure decreases with increasing deuterium number. The vapor pressures for $^{12}\mathrm{CH_4}$, $^{12}\mathrm{CH_3D}$, and $^{12}\mathrm{CH_2D_2}$ are 11.75, 7.89 and 7.65 mbar, respectively [17]. The VPIE is accordingly 0.674 and 0.643 for $^{12}\mathrm{CH_3D}/^{12}\mathrm{CH_4}$ and

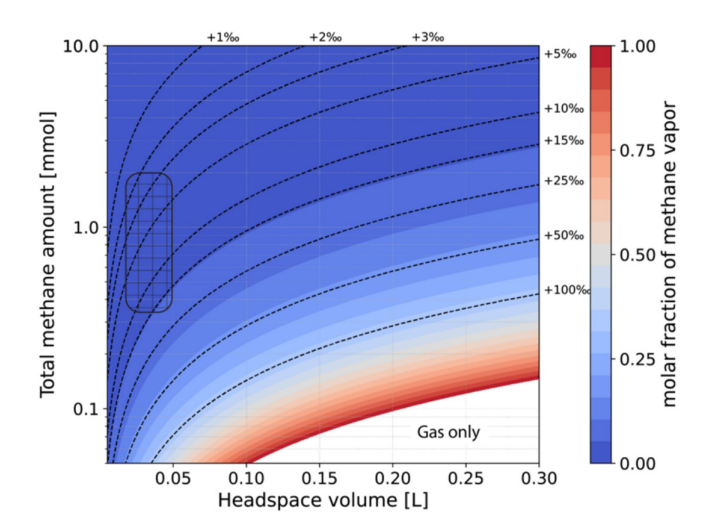


FIGURE 7 | Contour plot of the CH₄ molar vapor fraction at 77 K ice temperature with respect to total methane load and head space volume. Dashed lines represent the isopleths of $\Delta^{12}\text{CH}_2\text{D}_2$ excess in the methane ice due to the VPIE. The checkered field denotes the head space volume of vacuum lines used in this study and the typical total methane gas amounts processed in our QCLAS studies. Assuming full isotopic equilibration between the vapor and ice phase, as an example 40 mL (~1.8 mmol) methane handled in a vacuum line with 30 mL headspace are expected to experience up to ~3‰ excess $\Delta^{12}\text{CH}_2\text{D}_2$ in the ice phase. The relative uncertainty on the $\Delta^{12}\text{CH}_2\text{D}_3$ model results is 3.4%.

 $^{12}\text{CH}_2\text{D}_2/^{12}\text{CH}_4$ (see supplementary information for details, [17, 34]). To our knowledge, the vapor pressure for $^{13}\text{CH}_3\text{D}$ has not been determined. With the vapor pressures on hand, it is possible to conservatively estimate the relative enrichment of heavy methane isotopologues in the ice phase and calculate its $\Delta^{12}\text{CH}_2\text{D}_2$. Because of the normal isotope effect, the $\Delta^{12}\text{CH}_2\text{D}_2$ signature of fractionated ice will be positive, depicted as dashed lines in relation total amount of methane and vacuum line headspace volume in Figure 7. The calculation of the isotope effect was performed with the EP-06 isotopic composition, assuming equilibrium vapor-ice fractionation and considering a vacuum line temperature of 293 K. There is 3.4% relative uncertainty on the $\Delta^{12}\text{CH}_2\text{D}_2$ values if the vacuum line temperature varies $\pm 5\,\text{K}$.

Two observations can be made: (i) For the large methane amounts used in this study (40 mL or ~1.8 mmol), Δ^{12} CH₂D₂ excess is in the order of 1 to 4‰, depending on the vacuum line size (checkered field in Figure 7). The adsorbent-free experiments yield Δ^{12} CH₂D₂=0.9 ± 0.9‰, overlapping in error with the lower end of the theoretical excess. Considering that the interior volume of vacuum lines is usually smaller and the precision of $\Delta^{12}CH_2D_2$ measurements is in the range of 1%-5%, VPIE-induced shifts in $\Delta^{12}CH_2D_2$ for such large methane volumes become less significant. Thus, adsorbent-free trapping becomes a viable option. (ii) For moderate methane amounts, e.g., 1 mmol (22.4 mL gas, a typical sample volume used in our QCLAS system), the $\Delta^{12}CH_2D_2$ excess can be up to 12% for a vacuum line volume < 50 mL. For smaller methane volumes (~1-5 mL), commonly encountered in HR-IRMS applications, VPIE could introduce significant isotopic shifts of several tens of permil. For instance, a 0.1 mmol (2.24 mL) sample trapped in a 40 mL cryotrap (e.g.,

during gas transfer in a larger vacuum line) could experience a $\Delta^{12} \text{CH}_2 \text{D}_2$ shift of 56‰. In these cases, using adsorbents is integral to best preserving the clumped isotope signature of the methane sample.

Generally, downsizing internal vacuum line volumes while maximizing methane sample volume will reduce potential VPIE that could affect the clumped signature.

5 | Conclusions

This study systematically evaluated the performance of silica gels, zeolite molecular sieves, and activated carbon as cryogenic adsorbents for methane trapping and desorption in bulk and clumped isotope analyses. Emphasis was given to the ease of use of the adsorbent, where the (re-) conditioning procedure was constant at 160°C-180°C under a 10⁻³ mbar vacuum for at least 12 h. Silica gels demonstrated superior performance in preserving the isotopic integrity of methane. They exhibited minimal isotopic fractionation across δ^{13} C-CH₄, δ D-CH₄, Δ^{13} CH₃D, and $\Delta^{12}CH_2D_2$. Their relatively high adsorption capacity, ease of handling, and reproducibility make silica gels ideal for use in dead-end traps and other cryogenic applications. Zeolite molecular sieves and activated carbon showed variable performance, often introducing significant isotopic fractionations due to catalytic effects or chromatographic isotope separation, and thus should be carefully tested beforehand if applications require their use. Our experiments revealed that heating silica gel traps at higher temperatures (80°C and 95°C) could lead to inconsistencies in clumped isotope signatures, likely due to insufficient equilibration or catalytic effects. Heating coarsegrained (1-3 mm) silica gel at 50°C for 5 min was sufficient to reduce apparent isotope effects within performance targets, but best results for all isotope ratios were achieved for samples desorbing for at least 120 min at room temperature (21°C). Adsorbent-free cryotrapping offers a viable alternative if the methane sample is abundant and vacuum headspace volumes are low, and such vapor pressure isotope effects (VPIEs) become negligible. However, for most cases, cryogenic adsorbents remain essential to mitigate VPIEs and thus minimize isotopic shifts. We think that our study provides useful guidelines for using adsorbent materials in stable and clumped isotope geochemistry also beyond the methane system.

Author Contributions

Nico Kueter: conceptualization, project administration, formal analysis, methodology, visualization, writing – original draft. Naizhong Zhang: investigation, methodology, writing – review and editing. Jan G. C. Meissner: investigation, writing – review and editing. Léna Monnereau: visualization, investigation. Paul M. Magyar: methodology, writing – review and editing. Lukas Emmenegger: funding acquisition, supervision. Stefano M. Bernasconi: funding acquisition, writing – review and editing, supervision. Joachim Mohn: funding acquisition, methodology, writing – review and editing, supervision.

Acknowledgments

We thank Jordon Hemingway and Henner Busemann (both ETH Zurich) for providing adsorbent materials and Juliana Troch (RWTH Aachen) for fruitful discussions. We further thank two anonymous

reviewers for their helpful suggestions. This study is supported by the Swiss National Science Foundation project no. 200021-200977 (CLUMPME) and 206021_183294 (QCL4CLUMPS). This work is part of the project 21GRD04 isoMET, which has received funding from the EMPIR program cofinanced by the Participating States and from the European Union's Horizon Europe research and innovation program. The Empa contribution has received funding from the Swiss State Secretariat for Education, Research and Innovation (SERI). Open access publishing facilitated by Eidgenossische Technische Hochschule Zurich, as part of the Wiley - Eidgenossische Technische Hochschule Zurich agreement via the Consortium Of Swiss Academic Libraries.

Data Availability Statement

The data that supports the findings of this study are available in the supplementary material of this article.

Peer Review

The peer review history for this article is available at https://www.webofscience.com/api/gateway/wos/peer-review/10.1002/rcm.10040.

References

- 1. T. Giunta, E. D. Young, O. Warr, et al., "Methane Sources and Sinks in Continental Sedimentary Systems: New Insights From Paired Clumped Isotopologues $\rm ^{13}CH_{3}D$ and $\rm ^{12}CH_{2}D_{2}$," $Geochimica\ et\ Cosmochimica\ Acta\ 245\ (2019):\ 327–351.$
- 2. M. A. Haghnegahdar, J. Sun, N. Hultquist, et al., "Tracing Sources of Atmospheric Methane Using Clumped Isotopes," *Proceedings of the National Academy of Sciences of the United States of America* 120, no. 47 (2023): e2305574120.
- 3. X. Mangenot, A. Tarantola, J. Mullis, J. P. Girard, V. H. le, and J. M. Eiler, "Geochemistry of Clumped Isotopologues of $\mathrm{CH_4}$ Within Fluid Inclusions in Alpine Tectonic Quartz Fissures," *Earth and Planetary Science Letters* 561 (2021): 116792.
- 4. S. Eyer, B. Tuzson, M. E. Popa, et al., "Real-Time Analysis of δ^{13} C-and δ D-CH₄ in Ambient air With Laser Spectroscopy: Method Development and First Intercomparison Results," *Atmospheric Measurement Techniques* 9, no. 1 (2016): 263–280.
- 5. Y. Gonzalez, D. D. Nelson, J. H. Shorter, et al., "Precise Measurements of $^{12}{\rm CH_2D_2}$ by Tunable Infrared Laser Direct Absorption Spectroscopy," $Analytical\ Chemistry\ 91,\ no.\ 23\ (2019):\ 14967–14974.$
- 6. I. Prokhorov, B. Tuzson, G. Li, et al., Quantum Cascade Laser Spectrometer for Precise Measurements of $^{13}CH_3D$ and $^{12}CH_2D_2$. Optics and Photonics for Sensing the Environment (Optica Publishing Group, 2023): EM4E. 3.
- 7. N. Zhang, I. Prokhorov, N. Kueter, et al., "Rapid High-Sensitivity Analysis of Methane Clumped Isotopes (Δ^{13} CH $_3$ D and Δ^{12} CH $_2$ D $_2$) Using Mid-Infrared Laser Spectroscopy," *Analytical Chemistry* 97 (2025): 1291–1299.
- 8. N. Z. Zhang, G. T. Snyder, M. Lin, et al., "Doubly Substituted Isotopologues of Methane Hydrate ($^{13}\mathrm{CH}_{3}\mathrm{D}$ and $\mathrm{CH}_{2}\mathrm{D}_{2}$): Implications for Methane Clumped Isotope Effects, Source Apportionments and Global Hydrate Reservoirs," *Geochimica et Cosmochimica Acta* 315 (2021): 127–151.
- 9. I. Prokhorov and J. Mohn, "CleanEx: A Versatile Automated Methane Preconcentration Device for High-Precision Analysis of $^{13}\mathrm{CH_4}$, $^{12}\mathrm{CH_3D}$, and $^{13}\mathrm{CH_4D}$," Analytical Chemistry 94, no. 28 (2022): 9981–9986.
- 10. C. Rennick, T. Arnold, E. Safi, et al., "Boreas: A Sample Preparation-Coupled Laser Spectrometer System for Simultaneous High-Precision in Situ Analysis of δC and δH From Ambient Air Methane," *Analytical Chemistry* 93, no. 29 (2021): 10141–10151.
- 11. M. Sivan, T. Röckmann, C. van der Veen, and M. E. Popa, "Extraction, Purification, and Clumped Isotope Analysis of Methane ($\Delta^{13}\text{CDH}_3$ and $\Delta^{12}\text{CD}_2\text{H}_2$) From Sources and the Atmosphere," *Atmospheric Measurement Techniques* 17, no. 9 (2024): 2687–2705.

- 12. P. A. De Groot, *Handbook of Stable Isotope Analytical Techniques, 1* (Elsevier, 2004).
- 13. D. L. Eldridge, R. Korol, M. K. Lloyd, et al., "Comparison of Experimental vs Theoretical Abundances of $^{13}\text{CH}_3\text{D}$ and $^{12}\text{CH}_2\text{D}_2$ for Isotopically Equilibrated Systems From 1 to 500°C ," *ACS Earth and Space Chemistry* 3, no. 12 (2019): 2747–2764.
- 14. E. D. Young, I. E. Kohl, B. S. Lollar, et al., "The Relative Abundances of Resolved $^{12}\mathrm{CH}_2\mathrm{D}_2$ and $^{13}\mathrm{CH}_3\mathrm{D}$ and Mechanisms Controlling Isotopic Bond Ordering in Abiotic and Biotic Methane Gases," *Geochimica et Cosmochimica Acta* 203 (2017): 235–264.
- 15. H. R. Karlsson, *The Use of Molecular Sieves in Stable Isotope Analysis, Handbook of Stable Isotope Analytical Techniques* (Elsevier, 2004): 805–819.
- 16. D. A. Stolper, A. L. Sessions, A. A. Ferreira, et al., "Combined ¹³C-D and D-D Clumping in Methane: Methods and Preliminary Results," *Geochimica et Cosmochimica Acta* 126 (2014): 169–191.
- 17. G. T. Armstrong, F. G. Brickwedde, and R. B. Scott, "Vapor Pressures of the Methanes," *Journal of Research of the National Bureau of Standards* 55, no. 1 (1955): 39–52.
- 18. A. Schimmelmann, 2024. "Indiana University Bloomington Schimmelmann Research Reference Materials."
- 19. N. Kueter, M. W. Schmidt, M. D. Lilley, and S. M. Bernasconi, "Experimental Determination of Equilibrium CH₄-CO₂-CO Carbon Isotope Fractionation Factors (300°C–1200°C)," *Earth and Planetary Science Letters* 506 (2019): 64–75.
- 20. L. V. McCarty and E. W. Balis, "The Contamination of Liquid Nitrogen by Oxygen of the air," *Chemical & Engineering News Archive* 27, no. 37 (1949): 2612.
- 21. M. Mohnke and J. Heybey, "Gas Solid Chromatography on Open-Tubular Columns An Isotope Effect," *Journal of Chromatography* 471 (1989): 37–53.
- 22. N. Kueter, M. W. Schmidt, M. D. Lilley, and S. A. Bernasconi, "Kinetic Carbon Isotope Fractionation Links Graphite and Diamond Precipitation to Reduced Fluid Sources," *Earth and Planetary Science Letters* 529 (2020): 115848.
- 23. B. De Darwent, 1970. "Bond Dissociation Energies in Simple Molecules," NSRDS-NBS 31.
- 24. G. J. Kramer, R. A. Vansanten, C. A. Emeis, and A. K. Nowak, "Understanding the Acid Behavior of Zeolites From Theory and Experiment," *Nature* 363, no. 6429 (1993): 529–531.
- 25. J. A. Lercher and K. Seshan, "Sorption and Activation of Hydrocarbons by Molecular Sieves," *Current Opinion in Solid State & Materials Science* 2, no. 1 (1997): 57–62.
- 26. B. Schoofs, J. A. Martens, P. A. Jacobs, and R. A. Schoonheydt, "Kinetics of Hydrogen-Deuterium Exchange Reactions of Methane and Deuterated Acid FAU- and MFI-Type Zeolites," *Journal of Catalysis* 183, no. 2 (1999): 355–367.
- 27. A. C. Turner, R. Korol, D. L. Eldridge, et al., "Experimental and Theoretical Determinations of Hydrogen Isotopic Equilibrium in the System $\mathrm{CH_4}$ - $\mathrm{H_2}$ - $\mathrm{H_2}$ O From 3 to 200°C," *Geochimica et Cosmochimica Acta* 314 (2021): 223–269.
- 28. A. Sattler, "Hydrogen/Deuterium (H/D) Exchange Catalysis in Alkanes," *ACS Catalysis* 8, no. 3 (2018): 2296–2312.
- 29. W. Meier-Augenstein, A. Hess, G. F. Hoffmann, and D. Rating, "Evaluation of Water Removal and Memory Effect in $^{13}\mathrm{CO}_2$ Breath Tests by Isotope Ratio Mass-Spectrometry," *Isotopenpraxis* 30, no. 4 (1994): 349–358.
- 30. H. R. Karlsson and R. N. Clayton, "Oxygen Isotope Fractionation Between Analcime and Water—An Experimental Study," *Geochimica et Cosmochimica Acta* 54, no. 5 (1990): 1359–1368.

- 31. R. T. Yang, Gas Separation by Adsorption Processes, 1 (World Scientific, 1997).
- 32. E. M. Robson, "The Vacuum Use of Molecular Sieves and Other Desiccants," *Vacuum* 11, no. 1 (1961): 10–15.
- 33. B. M. Van Vliet, "The Regeneration of Activated Carbon," *Journal of the South African Institute of Mining and Metallurgy* 91, no. 5 (1991): 159–167.
- 34. G. Jancso and W. A. Van Hook, "Condensed Phase Isotope-Effects (Especially Vapor-Pressure Isotope-Effects)," *Chemical Reviews* 74, no. 6 (1974): 689–750.

Supporting Information

Additional supporting information can be found online in the Supporting Information section. $\,$